COMMUNICATION

Synthesis of chalcogenide ternary and quaternary nanotubes through directed compositional alterations of bacterial As–S nanotubes†

Shenghua Jiang,[a] Fang Liu,[b] Min-Gyu Kim,[c] Jae-Hong Lim,[b] Kun-Jae Lee,[d] Yong-Ho Choa,[d] Kyung Song,[e] Michael J. Sadowsky,[f] Wilfred Chen,[b] Nosang V. Myung*[b] and Hor-Gil Hur*[a]

Chalcogenide ternary (*i.e.* As–S–Se and As–Cd–S) and quaternary (*i.e.* As–Cd–S–Se) composite nanotubes were synthesized using biotic As–S nanotubes as template structures through bacterial Se(IV) reduction by *Shewanella* sp. HN-41 and/or abiotic cation exchange of As–S with Cd under ambient conditions.

Semiconducting nanostructures have become intensively investigated by both experimentalists and theoreticians because of their unique size dependent electronic and optical properties.[1] One group of the most investigated semiconductors is chalcogenide compounds (MX, M = As, Cd, Zn; X = S, Se, Te) because their band gap can be easily fine-tuned from zero (like the semi-metal HgTe) to a large band gap (*e.g.* ZnS (E_g = 3.8 eV)).[2] Recently, diverse one-dimensional (1D) chalcogenide nanostructures including the semiconducting nanowires and nanotubes have been synthesized and used as important building blocks for many potential applications.[3–5] However, majority of the nanostructures were synthesized through chemical or physical methods which typically require harsh reaction conditions such as high operating temperature, extremely high or ultra-low pressure, catalyst and toxic precursors.[5–8] In contrast, bio-inspired or biomimic routes allow synthesizing nanoengineered materials with "greener" precursors under mild ambient conditions.[9,10]

It is well-known that microorganisms play essential roles in the biogeochemical cycling of elements and in the formation of unique minerals/materials[11–13] through altering the valence/oxidation state of heavy metals and metalloids for anaerobic respiration.[14–16] Recent research has shown new insight on the reducing capabilities of certain anaerobic bacteria which offer significant utility in both heavy metal remediation and nano-manufacturing.[17–19] Among the bacteria, *Shewanella* strains have been shown to contribute to the formation of diverse nano-scaled minerals by virtue of their respiratory mechanisms.[3,20,21] For example, *Shewanella* sp. HN-41 showed the biological synthesis of one-dimensional As–S nanotubes which exhibited photoactive and semiconducting properties *via* the reduction of As(v) and thiosulfate under ambient anaerobic culture conditions.[3]

It has been reported that diverse semiconducting inorganic hybrid nanotubes were synthesized *via* ion exchange reaction to enhance the functionality and applicability.[22–24] It is also known that electrical conduction is closely associated with the structures such as the grain size, defects and impurities. Especially, the conduction of semiconductors is mainly governed by the grain boundary scattering where amorphous/nanocrystalline materials have much lower carrier concentration and mobility than single or polycrystalline materials with larger grains.[25] As the grain size increased, the contribution of grain resistance would be reduced, resulting in smaller thermal activation energy, E_A.[26] This suggested that the biologically photoactive As–S nanotubes can be transformed into tunable structures with varying compositions and ideal electrical property *via* kinetically controlled solution-phase ion exchange reaction and crystallization.

Thus, in this study, various biological activities of dissimilatory metal-reducing bacteria, including the reduction of Se(IV) and the formation of the photoactive As–S nanotubes, were applied for the synthesis of the versatile ternary and quaternary chalcogenide (*i.e.* As–S–Se, As–Cd–S and As–Cd–S–Se) nanotubes with the aid of biological and/or abiological activities. Se and/or Cd were incorporated either by biogenic deposition or ion exchange onto As–S nanotubes to control their electrical properties, which may open-up the possibility to integrate these nanotubes in nanoelectronics, optoelectronics, and solar cells. The mineralogical, crystal structure, morphology and electrical properties of the nanotubes were characterized, thereby understanding the influence of the ratio and different elemental compositions.

Shewanella sp. HN-41 produced the As–S nanotubes *via* concomitant reduction of As(v) to As(III) and $S_2O_3^{2-}$ to S^{2-} when both 5 mM As(v) and 5 mM thiosulfate were present in the anaerobic medium as previously described.[3] The purified As–S nanotubes were resuspended in the same medium supplemented with 10 mM lactate and 2 mM sodium selenite as the electron donor and acceptor, respectively. After 24 h incubation with the bacterial inoculum, the concentration of dissolved Se in the culture decreased from 2 to

aDepartment of Environmental Science and Engineering, Gwangju Institute of Science and Technology, Gwangju, 500-712, Republic of Korea. E-mail: hghur@gist.ac.kr; Fax: +82-062-970-2434; Tel: +82-062-970-2437
bDepartment of Chemical and Environmental Engineering, University of California at Riverside, CA, 92521, USA. E-mail: myung@engr.ucr.edu; Fax: +1-951-827-5696
cPohang Accelerator Laboratory, Pohang, 790-784, Republic of Korea
dDepartment of Fine Chemical Engineering, Hanyang University, Ansan, 426-791, Republic of Korea
eKorea Basic Science Institute, Daejeon, 305-333, Republic of Korea
fDepartment of Soil, Water, and Climate, BioTechnology Institute, University of Minnesota, St. Paul, MN, 55108, USA

This journal is © The Royal Society of Chemistry 2011

J. Mater. Chem., 2011, **21**, 10277–10279 | 10277

0.9 mM (Fig. 1a) and a filamentous product with smooth surface morphology was formed (Fig. 1b and d). Cross-sectional TEM images showed tube features and EDX line profile analysis showed the presence of As, S and Se in a ratio of 2 : 1 : 2 (Fig. 1c) whereas the ratio of As : S in the As–S nanotubes was 2 : 3. These results implied that the sulfur in the As–S nanotubes was replaced by Se and the composition of the As–S–Se nanotubes can be tuned as $As_2S_xSe_{3-x}$ depending on the different reaction rates. Since it has been reported that some bacteria including *Shewanella oneidensis* can reduce Se(IV), through Se(0), down to Se(−II),[27-29] sulfur in the As–S nanotubes appeared to be replaced by Se(−II) which was produced by *Shewanella* sp. HN-41. In order to observe an oxidation state of selenium in the synthesized nanotubes, the XANES peak feature of the Se-ion exchanged nanotube is compared to those of standards Se(IV) and Se(−II) (ESI, Fig. S5a†). As shown in the ESI, Fig. S5a†, the main peak of the Se K-edge data from our samples (As–S–Se nanotubes) and the commercially available reference sample (As_2Se_3 powder) appeared at approximately 12 658 eV which is identical with previously reported As_2Se_3 from chalcogenide films,[30] and clearly showed a different absorption peak position as compared to that of Na_2SeO_3 (Se(IV)). This result suggested that sulfur in the biogenic As–S nanotubes can be replaced by Se(−II) through the reduction of Se(IV) by bacterial culture under anaerobic conditions.

In contrast to As–S–Se, the As–Cd–S nanotubes were synthesized through an abiotic process. The purified As–S nanotubes were resuspended in 2 mM $CdCl_2$ solution. A filamentous product with rough surface morphology (Fig. 2b and d) was formed and the concentration of Cd in the liquid phase decreased from 2 to 0.4 mM coupled to increase of As from 0 mM to 1.1 mM (Fig. 2a) after 2 h incubation. EDX line profile analysis of the tubular structure showed that the ratio of As, Cd and S was approximately 1 : 4 : 5 (Fig. 2c). The significantly lower ratio of As/S indicated Cd incorporation into the As–S nanotubes *via* cation exchange reaction. XRD spectral analysis showed several diffraction peaks of CdS with the preferred crystal orientation in the (444) and (107) direction (ESI, Fig. S3b†). Similar to Se anionic exchange process, Cd K-edge XANES characterization for the As–Cd–S nanotube directly presents successful ion-exchange reaction between host arsenic and guest cadmium ions (ESI, Fig. S5b†).
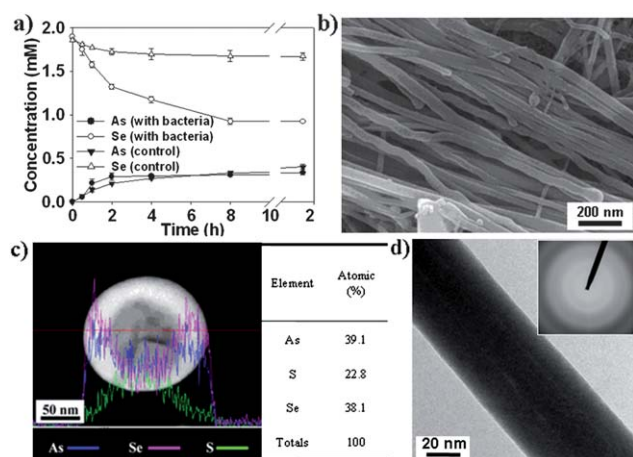

Fig. 2 Concentration of As and Cd in the solution (a), SEM image (b), EDX line profile across the cross-section (c), and HR-TEM image with SAED pattern (d).

Furthermore, consecutive Cd and Se dual-ion exchange can be successfully performed for the As_2S_3 nanotube to synthesize quaternary As–Cd–S–Se nanotubes. The As–Cd–S synthesized *via* cation As/Cd exchange reaction was purified and resuspended in the medium containing bacteria, lactate and Se(IV). After 24 h incubation, the concentration of soluble Se decreased from 2 to 1.2 mM (Fig. 3a) and the product with similar rough surface shape was formed (Fig. 3b and d). The EDX line profile analysis of the tubular structure showed that the ratio of As, Cd, S and Se was about 1 : 4 : 4 : 1 (Fig. 3c). The Cd and Se K-edge XANES after dual-ion exchange only showed a Se–As chemical interaction without any Se–Cd chemical bonding, whereas those for the Cd ion directly present distinct Cd–S chemical interaction and an absence of Cd–Se bonding (ESI, Fig. S5c†). This fact indicated that after the first Cd cationic exchange, the second Se anionic exchange occurred not in the Cd site but only the As site. As a result, there coexist arsenic sulfide, cadmium sulfide and arsenic selenide phases in the As–Cd–S–Se nanotube.

In determining the electric properties of the synthesized nanostructures, the temperature coefficient of the resistance (TCR) and

Fig. 1 Concentration of As and Se in the medium containing *Shewanella* sp. HN-41 (a), SEM image (b), EDX line profile across the cross-section (c), and HR-TEM image with SAED pattern (d).
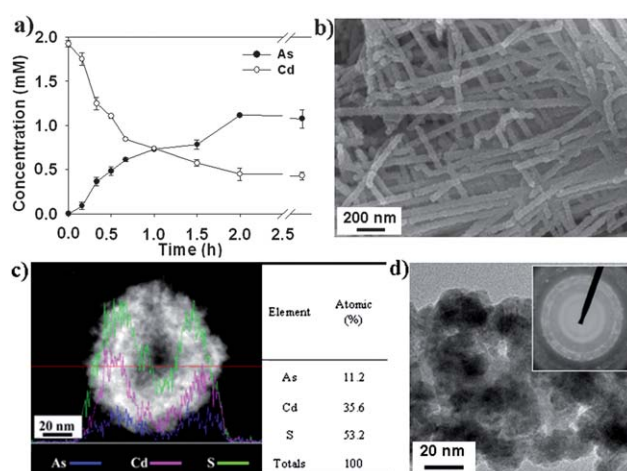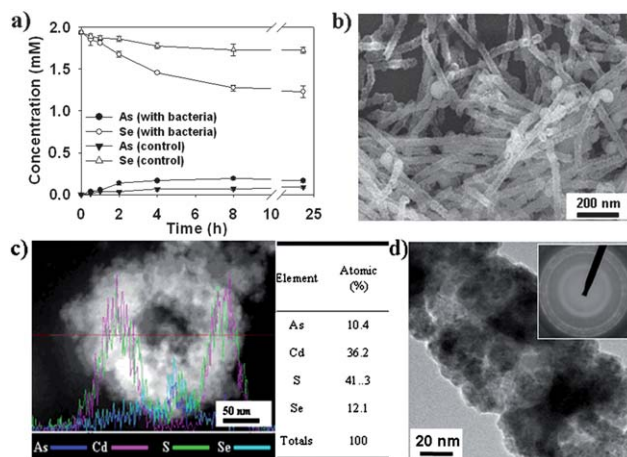

Fig. 3 Concentration of As and Se in the medium containing *Shewanella* sp. HN-41 (a), SEM image (b), EDX line profile across the cross-section (c), and HR-TEM image with SAED pattern (d).
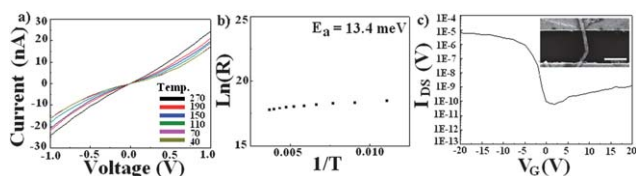
Fig. 4 Electrical characteristics of the As–Cd–S nanotubes. Temperature dependent I–V curves (a), electrical resistance change as a function of temperature (b), FET transfer characteristics with inset SEM image of aligned As–Cd–S nanotubes between electrode pads (scale bar: 1 μm) (c).

field effect transfer characteristics were measured. Prior to electrical measurement, the synthesized nanostructures were assembled across microfabricated gold electrodes. Fig. 4a–c show typical I–V characteristics of single As–Cd–S nanotubes.

At 270 K, As–Cd–S network showed almost linear I–V characteristics (Fig. 4a), indicating that the As–Cd–S nanotubes formed an ohmic contact. However, as the temperature decreased, the I–V curves became non-linear which might be caused by the decrease of the carrier concentration resulting from lower tunneling probability. Fig. 4b shows the temperature dependent resistance. The small activation energy of 13.4 meV was obtained from 270 to 210 K from the As–Cd–S nanotubes which implied a low density of deep charge traps and subsequent high channel conductivity. To further investigate the electrical properties, FET transfer characteristics were measured. As shown in Fig. 4c, the source–drain current (I_{DS}) was strongly dependent on the gate bias where a clear off-state was observed at positive bias voltage. From these results it can be inferred that the As–Cd–S nanotubes are p-type semiconductors with the carrier concentration and field effect mobility of $1.1 \pm 0.4 \times 10^{10}$ cm^{-1} and 0.08 ± 0.01 cm^2 V^{-1} s^{-1}, respectively (ESI, Fig. S9b†). Similar analysis was performed on the As–S, As–S–Se, and As–Cd–S–Se nanotubes which are shown in the ESI, Fig. S6, S7, and S8†, respectively. The comparison of their electrical properties is summarized in the ESI, Fig. S9† which clearly indicated the electrical properties can be tuned by controlling the composition of nanotubes.

In summary the, chemical composition of the biogenic photoactive As–S nanotubes can be tuned by biological and abiological processes under environmentally benign conditions, producing the chalcogenide ternary and quaternary nanotubes by the incorporation of Cd and/or Se into their nanotube structures. This rapid, conditional, selective, and tunable synthesis can provide new opportunities to develop composition and structure dependent nanomaterials and tune their chemical/physical properties, which ultimately may find use in novel nano- and opto-electronic devices.

Acknowledgements

Notes and references

1 J. Hu, L. S. Li, W. Yang, L. Manna, L. W. Wang and A. P. Alivisatos, *Science*, 2001, **292**, 2060–2063.
2 T. Trindade, P. O'Brien and N. L. Pickett, *Chem. Mater.*, 2001, **13**, 3843–3858.
3 J.-H. Lee, M.-G. Kim, B. Yoo, N. V. Myung, J. Maeng, T. Lee, A. C. Dohnalkova, J. K. Fredrickson, M. J. Sadowsky and H.-G. Hur, *Proc. Natl. Acad. Sci. U. S. A.*, 2007, **104**, 20410–20415.
4 C. N. R. Rao and M. Nath, *Dalton Trans.*, 2003, 1–24.
5 C. N. R. Rao and A. Govindaraj, *Adv. Mater.*, 2009, **21**, 4208–4233.
6 S. Chakrabortty, J. A. Yang, Y. M. Tan, N. Mishra and Y. Chan, *Angew. Chem., Int. Ed.*, 2010, **49**, 1–6.
7 J. C. Chen, Z. H. Lin and X. X. Ma, *Lett. Appl. Microbiol.*, 2003, **37**, 105–108.
8 M. Law, J. Goldberger and P. Yang, *Annu. Rev. Mater. Res.*, 2004, **34**, 83–122.
9 P. Mohanpuria, N. K. Rana and S. K. Yadav, *J. Nanopart. Res.*, 2008, **10**, 507–517.
10 A. Ahmad, P. Mukherjee, S. Senapati, D. Mandal, M. I. Khan, R. Kumar and M. Sastry, *Colloids Surf., B*, 2003, **28**, 311–318.
11 D. Fortin, *Science*, 2004, **303**, 1618–1619.
12 H. A. Lowenstam, *Science*, 1981, **211**, 1126–1131.
13 D. K. Newman, *Science*, 2001, **292**, 1312–1313.
14 Y. A. Gorby and D. R. Lovley, *Appl. Environ. Microbiol.*, 1991, **57**, 867–870.
15 D. R. Lovley, *Microbiol. Rev.*, 1991, **55**, 259–287.
16 J. K. Fredrickson, H. M. Kostandarithes, S. W. Li, A. E. Plymale and M. J. Daly, *Appl. Environ. Microbiol.*, 2000, **66**, 2006–2011.
17 C. T. Dameron, R. N. Reese, R. K. Mehra, A. R. Kortan, P. J. Carroll, M. L. Steigerwald, L. E. Brus and D. R. Winge, *Nature*, 1989, **338**, 596–597.
18 D. R. Lovley, J. F. Stolz, G. L. Nord and E. J. P. Phillips, *Nature*, 1987, **330**, 252–254.
19 T. C. Ho, J. W. Kim, W. B. Kim, K. Song, R. A. Kanaly, M. J. Sadowsky and H.-G. Hur, *J. Mater. Chem.*, 2010, **20**, 5899–5905.
20 J. H. Lee, J. H. Han, H. C. Choi and H.-G. Hur, *Chemosphere*, 2007, **68**, 1898–1905.
21 S. Jiang, J. H. Lee, M. G. Kim, N. V. Myung, J. K. Fredrickson, M. J. Sadowsky and H. G. Hur, *Appl. Environ. Microbiol.*, 2009, **75**, 6896–6899.
22 D. H. Son, S. M. Hughes, Y. Yin and A. Paul Alivisatos, *Science*, 2004, **306**, 1009–1012.
23 R. D. Robinson, B. Sadtler, D. O. Demchenko, C. K. Erdonmez, L. W. Wang and A. P. Alivisatos, *Science*, 2007, **317**, 355–358.
24 X. Duan, Y. Huang, R. Agarwal and C. M. Lieber, *Nature*, 2003, **421**, 241–245.
25 T. Minami, *MRS Bull.*, 2000, **25**, 38–44.
26 M. C. Kum, B. Y. Yoo, Y. W. Rheem, K. N. Bozhilov, W. Chen, A. Mulchandani and N. V. Myung, *Nanotechnology*, 2008, **19**, 325711–325718.
27 C. I. Pearce, V. S. Coker, J. M. Charnock, R. A. D. Pattrick, J. F. Mosselmans, N. Law, T. J. Beveridge and J. R. Lloyd, *Nanotechnology*, 2008, **19**, 155603.
28 R. S. Oremland, M. J. Herbel, J. S. Blum, S. Langley, T. J. Beveridge, P. M. Ajayan, T. Sutto, A. V. Ellis and S. Curran, *Appl. Environ. Microbiol.*, 2004, **70**, 52–60.
29 C. I. Pearce, R. A. Pattrick, N. Law, J. M. Charnock, V. S. Coker, J. W. Fellowes, R. S. Oremland and J. R. Lloyd, *Environ. Technol.*, 2009, **30**, 1313–1326.
30 M. Popescu, F. Sava, N. Aldea, X. Yaning, H. Tiandou, L. Tao and M. Leonovici, *Chalcogenide Lett.*, 2005, **2**, 71–76.